The impedance of hydrogen oxidation reaction in a proton exchange membrane fuel cell in the presence of carbon monoxide in hydrogen stream

K. Darowicki [a], L. Gawel [a],[*], M. Mielniczek [a], A. Zielinski [a], E. Janicka [a], J. Hunger [b], L. Jorissen [b]

[a] Department of Electrochemistry, Corrosion and Materials Engineering, Chemical Faculty, Gdansk University of Technology, 11/12 Narutowicza, 80-233 Gdansk, Poland
[b] Zentrum für Sonnenenergie- und Wasserstoff-Forschung Baden-Württemberg (ZSW) Helmholtzstraße 8, 89081 Ulm, Germany

HIGHLIGHTS

- Carbon monoxide pollution of hydrogen stream.
- On-line impedance changes of anode exposed to different concentrations of carbon monoxide.
- Evaluation of carbon monoxide surface coverage of anodic catalyst.
- Coherence between AC and DC measurements by self- validation methodology.

ABSTRACT

Evaluation of performance of a proton exchange membrane fuel cell, which is affected by carbon monoxide that pollutes the hydrogen stream, was presented. This influence was studied for carbon monoxide concentration of 125–325 ppb, which are close to values specified in ISO 14687:2019 standard. Performed studies provided crucial information for further development of fuel cell as an energy source for automotive application. Impedance with the use of Dynamic Electrochemical Impedance Spectroscopy profile measurements were completed for chosen carbon monoxide concentration under a constant current load and anode impedance variations were determined as a function of the time exposed to carbon monoxide. A method to determine the impedance of hydrogen oxidation was proposed. It was determined how the carbon monoxide surface coverage of anodic catalyst varies as a function of time. The capacitance of the double electrical layer and the charge transfer resistance of anodic reaction are discussed to evaluate them with respect to exposure time and surface coverage. It has been shown that proposed methodology can be used as a universal tool for testing fuel cells for both research and industrial applications, with the overall aim of optimization, monitoring, and diagnostics of the fuel cell.

1. Introduction

Proton Exchange Membrane Fuel Cells (PEMFC) are called as the main energy source of the future. The main advantages of fuel cells as energy sources are producing high-density energies, generate net-zero harmful emissions [1] low-temperature operation, quick start-up, low noise and vibration [2,3]. They are already used in different vehicles types such as cars [4,5] and aircrafts [6] and others [7]. Unfortunately, one of the disadvantages of this devices is the requirement for high purity of applied hydrogen as a fuel. Maximum levels of contamination have been determined in the ISO 14687:2019 standard. For carbon

monoxide (CO) the limit value is determined to be 0.2 μmol/mol (200 ppb). Trace amounts of CO are found in the hydrogen fuel when produced in refineries during the reforming process [8]. Balasubramanian and Weidner with the use twin-cell electrochemical filter reduced CO from hydrogen reformate to the level of 10 ppm [9]. This CO contamination has serious consequences, as even trace quantities of CO in hydrogen poison platinised anodic catalysts, which are routinely used in PEMFC [10]. Platinum catalyst poisoning is caused by CO adsorption onto Pt centres which is preferred over adsorption of hydrogen. The influence of CO content on the HOR mechanism using the EIS technique was investigated by Wagner and Schulze [11]. Postole and Auroux

investigated the effect of CO in a hydrogen stream on platinum catalysts by applying the microcalorimetry technique [12]. The poisoning of the catalyst inhibits the dissociation of H_2 and adsorption of H_{AD}. The further stages of oxidation of hydrogen are consequently inhibited since the bond between platinum and CO is stronger than between Pt and hydrogen [13]. There are two types of bonds for adsorbed CO particles. The first is linearly adsorbed forms of carbon monoxide and these utilize one active centre on platinum, whereas the form of CO bridged with a Pt catalyst needs two active sites [10]. This was confirmed by the research carried out with the use of a rotating disc electrode by Igarashi et al. [14], and also by tests performed by Watanabe and Motoo on a polycrystalline electrode with the use of electrochemical pulse technique [15]. Fasmin and Ramanathan, using numerical simulation, performed a detailed kinetic analysis of impedance spectra during CO poisoning of the anode catalyst [16].

It is possible to remove carbon monoxide through direct oxidation forming carbon dioxide, with the reaction rate dependent on the adsorbed particles of OH_{AD}, which act as oxygen donors, which was described in the works of Neugebohren et al. [17] Zhang [18] and Wang et al. [19]. The forms containing oxygen are formed on the surface of platinum at a 500 mV potential vs. RHE. Alloying with a transition metal, such as Ru [20,21], Co, Mo, Pd [22], or Sn increases the tolerance of an anode catalyst to hydrogen contamination with CO by allowing the generation of active oxygen donors at a potential significantly lower than that of pure platinum [23,24]. The PtRu catalyst shows the most promising CO tolerance amongst the two-component Pt alloy catalysts [25,26]. However, the electrochemical and chemical stability of PtRu catalysts is lower than that of pure Pt, what was presented by Taniguchi et al. [27], Sheng et. al. [28] and Wang et al. [29].Continuous improvement and development of stable anode catalysts which are highly active against oxidation of hydrogen and excellent tolerance to CO are of paramount importance in commercialising PEMFC. For this reason, authors proposed methodology, which allows evaluating the sensitivity of the catalyst to CO and look into the possibility of continuous diagnostics of anode status when a cell actually operates.

To evaluate the tolerance of a fuel cell to contamination with carbon monoxide under laboratory conditions, researchers use electrochemical impedance spectroscopy (EIS). Nakajima, et al. tested a fuel cell with the supply of hydrogen contaminated with CO by performing current-voltage characteristics and EIS measurements [30]. Tang et al. used the EIS technique to prove the improved tolerance to the presence of CO in the fuel of the PdPt electrocatalyst compared to pure Pt catalyst [31]. Ciureanu and Wang proved that the impedance spectra of the poisoned electrode are strongly dependent on the potential and concentration of CO in the feed gas [32]. Chandesris et al. investigated the heterogeneity of degradation in the PEMFC stack under the influence of CO poisoning using the EIS technique [33]. The materials electrical impedance is analysed by applying an equivalent circuit model comprising of several resistances and capacitances that are assigned to activation, diffusion and, adsorption/desorption. Values of capacitance have been shown to depend among others on the density of the generated current, the surface area of catalysts, anode potential and the amount of CO in the supplied fuel [30]. The EIS technique is also routinely used to monitor commercial fuel cells, as described in extensive reviews [34,35,36]. Giner-Sanz et al. used the spectra obtained with the EIS technique to mechanistic equivalent circuit modelling of a commercial polymer electrolyte membrane fuel cell [37].

Unfortunately, the use of EIS under varying conditions of on-line cell operation is not possible. Dynamic electrochemical impedance spectroscopy (DEIS) is not limited in terms of the stationary nature of the investigated process. A detailed description of DEIS and limitation of EIS method in comparison to DEIS has been previously presented in a number of publications [38,39,40]. This technique has been successfully used in: measuring impedance changes during dynamic load changes [41] and humidity changes [42], in fault detection of PEM fuel cell stacks [43], characterization of other power sources such as direct

methanol fuel cells [44] and methanol fuel cell stacks [45], in-situ measurements of DMFC cathode impedance [46] and others [47,48].

This paper is focused on using DEIS to assess the influence of hydrogen polluted with carbon monoxide on the cell operating conditions. This is an innovative approach, which allows to continuously diagnose the cell. Diagnosis of anode catalytic activity under operating conditions is a complex issue that has not been previously investigated. An instantaneous change in the anode impedance due to carbon monoxide poisoning was demonstrated. In addition to identifying the hydrogen oxidation impedance, the process of correct determining of impedance is another equally important problem. In measuring the impedance, there are always issues with verifying the uniqueness of the analyses and assessing its validity. Therefore, an additional objective is to determine the criterion of the measurement validity. Achieving these objectives is of key importance for diagnostics and monitoring of the anode process in the operation of a cell. The paper also shows the possible applications of DEIS in the diagnostics and monitoring of fuel cells.

2. Materials and methods

The experiments were carried out on a single PEM fuel cell engineered by ZSW (Ulm, Germany), with an active surface area of 47 cm^2 with Pt/C catalyst. The cell was built using MEA in automotive purposes, which has a very low thickness and high attainable current density. The operating parameters were controlled using a ZSW test station which allowed for adjustment of all input and output operating parameters. The operating parameters were identical for all the tests performed. The cell temperature was controlled to 70 °C degrees, and the inlet gases were preheated to 72 °C. The fuel used was hydrogen with a purity of 5.0 and relative humidity of 35%, supplied in a stoichiometric excess of 1.4 at a pressure of 1.7 bar. The oxidant feed was composed of compressed air with a relative humidity of 60% in a stoichiometric excess of 1.6 at a pressure of 1.4 bar. All values of operating parameters were specified and set at the inlet. Impedance testing was completed using a module from National Instruments (Texas, USA) equipped with a PXIe-5413 signal generator and a PXIe-4464 data acquisition card. The program for testing and analysis of impedance was written in LabView.

Measurements were performed at a current density of $j = 2$ Acm^2 with all constant parameters of cell operation, which is nominal current specified by manufacturer. For the first half an hour, all measurements were performed for a cell operating with the parameters, given above. After half an hour, the stream of hydrogen was supplied with a controlled amount of CO at the following concentrations: 0, 125, 250, and 325 ppb. CO was flowed towards the anode for 2.4 h at each concentration. After each poisoning, the cell was shut down for 12 h and then the anode was reactivated. During the cell operation, measurement of the DEIS was conducted continuously using a multi-sine current excitation signal with an effective amplitude of 5% of the DC load. This signal was composed of 32 elementary sine signals at frequencies ranging from 3 Hz to 20 kHz with adequately optimized amplitudes and phase shifts of each component. The obtained impedance spectra were analysed in detail using an equivalent circuit which is thoroughly described in the Results and Discussion section (*vide-infra* 3.1 and 3.2 section).

3. Results and Discussion

3.1. Chrono-impedance of a fuel cell supplied with pure hydrogen

The pure hydrogen fuel cell was tested with a controlled direct current and a constant supply of oxygen and hydrogen to the cathode and anode, respectively. The operating temperature and wetting were stabilized to comply with the values described in Materials and Methods. The resulting chrono-impedance graph is shown in Fig. 1.

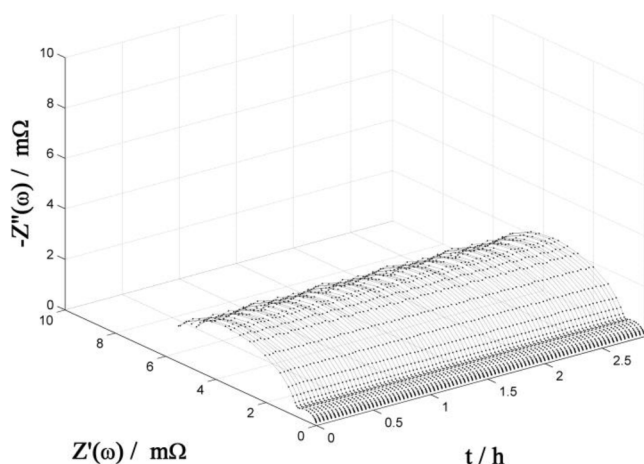The chrono-impedance plot is a composition of the elementary

Fig. 1. A chrono-impedance plot of a hydrogen fuel cell obtained for a constant current load j = 2 Acm2 with the absence of CO.

impedance of each spectra. Each individual impedance spectrum takes the form of two semi-circles. The isofrequential points on a chrono-impedance plot are arranged on parallel lines. This indicates that the cell's operation is stationary. The individual spectra of a chrono-impedance plot were analysed for correlation using a nonlinear method of least squares. The analysis used the following theoretical formula for impedance:

$$Z(t, 2j\pi f) = R_\infty + \frac{R_M}{1 + 2j\pi f C_M R_M} + \frac{R_{CT}^C}{1 + 2j\pi f C_{DL}^C R_{CT}^C} \qquad (1)$$

where: $Z(t, 2j\pi f)$ – cell impedance, R_∞ – the resistance of an electric circuit and the resistance of an anodic process, R_M – membrane resistance, R_{CT}^C – charge transfer resistance of cathodic reaction, C_M - membrane capacitance, and C_{DL}^C – the capacitance of electrical double layer of anode.

Cell impedance is the sum of membrane impedance and cathode impedance. In Eq. (1), the anode impedance is not included. This is due to the exchange current of oxidation/reduction of hydrogen is 2–3 orders of magnitude greater than the exchange current of oxidation/reduction of oxygen, what was proved in studies of Singh et al. [49] and Paulus et al. [50]. Additionally it was confirmed by Song et al. in studies

of kinetics of reactions taking place in PEM fuel cells in the range of 23–120 ° C [51]. From this, the impedance of the anodic process is 2–3 orders of magnitude lower than the impedance of the cathodic process [52]. Under normal operating conditions of a fuel cell, the anode impedance is negligibly small and only has minimal representation in the impedance spectra; its values can be considered as a component of the parameter R_∞.

Utilising correlation analysis, the achieved experimental spectra were fitted to the model of the system, given by 1, with fit quality expressed by χ^2. Over a duration of the experiment, χ^2 has no time dependence. The average goodness of fit was $\chi^2 \approx 6.210^{-4}$. The results of the correlation analysis are given in Fig. 2. The cell functioned under a stable regime. This is evidenced by the constant, time-independent electrochemical parameters of the fuel cell:

$$C_M = 65.98mF; \quad R_M = 0.83m\Omega; \quad C_{DL}^C = 1.43 \; F; R_{CT}^C = 4.71m\Omega$$

Relaxation of membrane and cathode occurs for certain frequency bands, which are characterized by resonance frequencies of the membrane and the cathodic reaction, which are given as:

$$f_M^* = 2905Hz; \quad f_C^* = 23Hz$$

where: f_M^* – the resonance frequency of a membrane, f_C^* – the resonance frequency of cathodic process

The resonance frequencies f_M^* and f_C^* have no dependence on the cell operating time. The impedance of the tested cell does not change under operating conditions, meaning energy is released from the cell in a stable way.

3.2. Chrono-impedance of a fuel cell supplied with hydrogen contaminated with carbon monoxide (CO)

After an exposure period of 30 mins under rated operating conditions, the stream of hydrogen feeding the anode was doped with carbon monoxide at concentrations ranging from 125 to 325 ppb. All cell operation parameters, such as temperature, relative humidity, gas flow rates were kept constant during the experiment without carbon monoxide. The chrono-impedance plots obtained for different carbon monoxide concentrations are shown in Figs. 3–5.

For a CO concentration of 125 ppb (Fig. 3), at the range of frequencies close to the lower limit and those close to the upper limit, the isofrequential lines are parallel. The elementary frequency spectra are
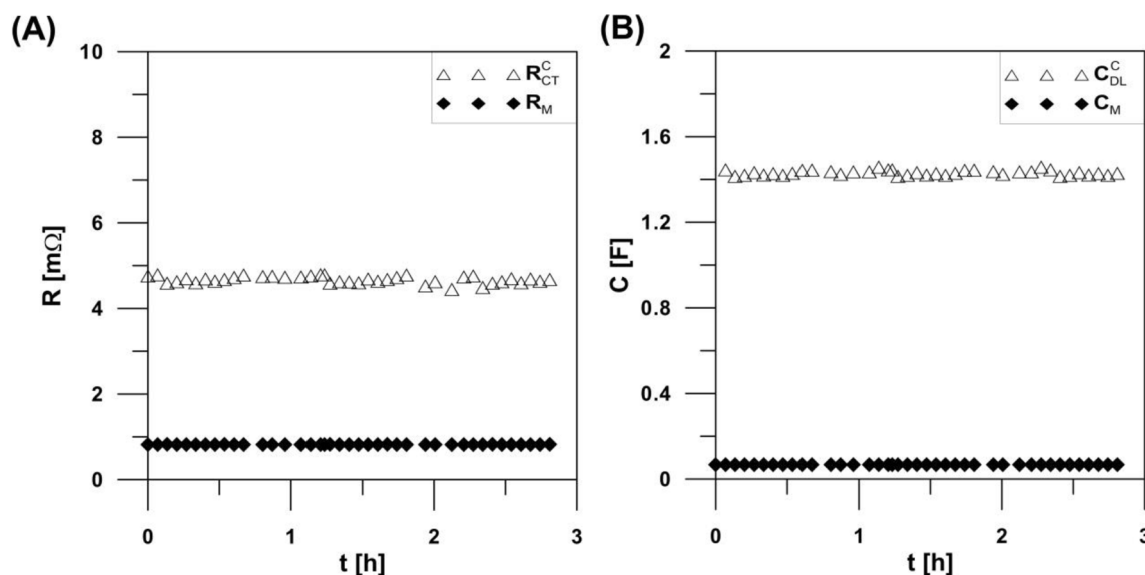

Fig.2. (A) The changes in membrane resistance and charge transfer resistance of the cathodic process. (B) Changes in the membrane capacitance and capacitance of the electrical double layer of anode. The cell was fed with pure hydrogen, without carbon monoxide.
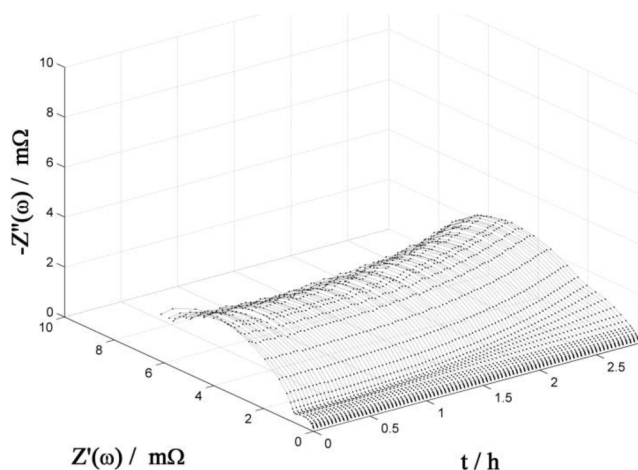
Fig. 3. A chrono-impedance plot of a hydrogen fuel cell obtained for a constant current load j = 2 Acm2 with the a carbon monoxide content of 125 ppb (post 30 mins) in the hydrogen stream.

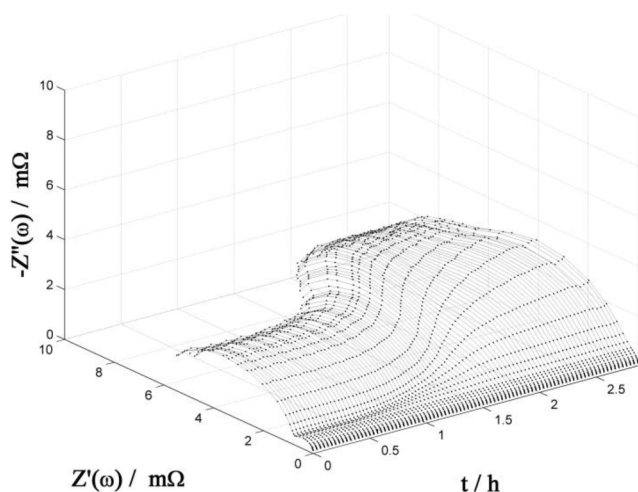**Fig. 4.** A chrono-impedance plot of a hydrogen fuel cell obtained for a constant current load j = 2 Acm2 with the a carbon monoxide content of 250 ppb (post 30 mins) in the hydrogen stream.

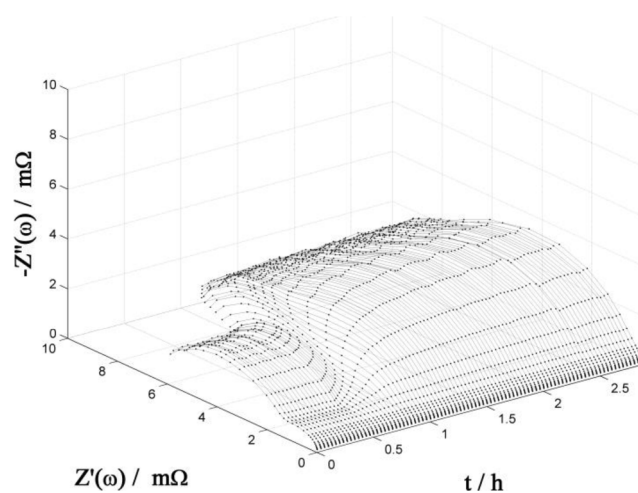**Fig. 5.** A chrono-impedance plot of a hydrogen fuel cell obtained for a constant current load j = 2 Acm2 with the a carbon monoxide content of 325 ppb (post 30 mins) in the hydrogen stream.

composed of two semi-circles, but after approximately one hour, the elementary impedance spectra start changing. Between the resonance frequencies $f_M^* = 2905Hz$; $f_C^* = 23Hz$, an additional process is observed, which becomes more visible with increased exposure of CO/H$_2$. Since only the conditions of hydrogen oxidation have been modified, a change in the spectrum is associated with the anodic processes. Therefore, these differences should be increasingly obvious with increasing concentration of carbon monoxide contamination of the hydrogen fuel feed.

Fig. 4 presents the chrono-impedance plot for a carbon monoxide concentration of 250 ppb. The increase in the content of CO in hydrogen amplifies the differences between the spectra identified at the beginning of the operation and the spectra corresponding to long-term exposure. Between the resonance frequencies $f_M^* = 2905Hz$; $f_C^* = 23Hz$, there is a clear, visible, emerging frequency band. This band is attributed to changes in the anodic processes. Over this frequency range, the non-stationary nature of the cell's operation begins. Two stationary states are observed. The first stationary state corresponds to the initial period of operation, that is $0.0 < t < 1.0h$. The second stationary state corresponds to the operation period from $2.0h < t < 2.8h$.

Between these stationary states, the impedance characteristics strongly depend on time of exposure. Impedance measurements over this time range using frequency-by-frequency techniques result in internally inconsistent (non-coherent) impedance spectra. Each frequency point of a single spectrum corresponds to a different time. For this reason, each frequency point corresponds to a different electrochemical state of the cell and a different degree of the catalyst being poisoned with CO. The non-stationary operation area should become clearly visible with an increased CO content in H$_2$.

The anodic frequency band is clearly more enhanced in Fig. 5. For a CO content of 325 ppb in H$_2$, the non-stationary area of the chrono-impedance plot is observable at an earlier stage and covers a period of $0.5h < t < 1h$. This chrono-impedance plot shows the diversity of the elementary impedance spectra. The forms of the spectra evolve from typical two-time constant spectra to more complex spectra. Elementary spectra for the initial period are radically different from the spectra identified at increased times. During the transitional range of times, the system is non-stationary. The relaxation processes that occur should be associated with hydrogen oxidation inhibited by carbon monoxide adsorption.

If carbon monoxide is present in the hydrogen, the impedance of the CO oxidation on the anode cannot be neglected. The impedance measured globally is the sum of the cathodic reaction impedance, the anodic reaction impedance, and the membrane impedance. Therefore, to perform a detailed correlation analysis of the achieved chrono-impedance plot, the following theoretical formula should be used:

$$Z(t, 2j\pi f) = R_\infty + \frac{R_M}{1 + 2j\pi f C_M R_M} + \frac{R_{CT}^C}{1 + 2j\pi f C_{DL}^C R_{CT}^C} + \frac{R_{CT}^A(t)}{1 + 2j\pi f C_{DL}^A(t) R_{CT}^A(t)}$$

(2)

where: $R_{CT}^A(t)$ – the charge transfer resistance of oxidation in the function of time, and $C_{DL}^C(t)$ – the capacitance of electrical double layer of anode in the function of time.

Due to a large number of variables being optimized; $R_\infty, R_M, R_{CT}^C, R_{CT)}^A(t), C_M, C_{DL}^C, C_{DL}^A(t)$, it is difficult to use a least square method directly, and the results obtained were inconsistent. The objective function determining the goodness of fit was $\chi^2 \approx 10^{-2}$, this was too low to give an satisfactory fitting. In addition, the obtained numerical values of the parameters being optimized did not change as a monotonic function of time, which is in contrast to the impedance spectra that change in a regular manner over chrono-impedance plots. Moreover, the iso-frequential lines are monotone, therefore, it was necessary to correct the correlation process in order to obtain more valid results. This modification was completed to reduce the number of degrees of freedom for the fit.

To simplify the problem, the fuel cell operation was first analysed. The cell operates in a galvanostatic mode and as a result, the stream of protons passing through the membrane is constant. The stream of oxygen reaching the cathode is also constant, along with the operating moisture and temperature. As a result, the impedance of oxygen reduction should not be time-dependent, as the process is stationary. Similarly, the membrane impedance should also be constant, irrespective of the CO content, as a constant stream of hydrogen cations passes through the membrane. This evaluation is observed by the chrono-impedance plot in Fig. 1. Under these conditions, the membrane impedance and the impedance of the reduction process do not vary over time, therefore the correlation formula gets simplified to:

$$Z(t, j2\pi f) = R_\infty + \frac{0.83}{1000 + j0.83 \cdot 65.98f} + \frac{4.71}{1000 + j4.71 \cdot 1460f}$$
$$+ \frac{R_{CT}^A(t)}{1 + 2j\pi f C_{DL}^A(t) R_{CT}^A(t)} \tag{3}$$

This causes the whole correlation process to reduce from being seven variables down to the two variables $R_{CT}^A(t)$ and $C_{DL}^A(t)$. This procedure has greatly improved the quality of the results obtained.

Fig. 6 shows the changes in the capacitance of the double electric layer of the anode catalyst with different content of carbon monoxide in the hydrogen. Over time, the capacitances of the double electrical layer decrease monotonically. An increase in the CO content in the hydrogen stream amplifies these changes. For higher concentrations of CO in hydrogen, the lowest values for the capacitance of the double electrical layer of the anode are observed. The capacitance of the electrical double layer does not change in a regular manner. For an initial period of $C_{DL}^A(t)$, the capacitance is constant as CO is absent from the stream. After relativity long exposures to CO, the value for the capacitance of anode electrical double layer again reaches a constant value approximate 0.25 F for all concentrations.

3.3. Electrocatalytic activity and anode poisoning by carbon monoxide

Oxidation of hydrogen is a multistep process. The first step of hydrogen oxidation is the chemical dissociation of hydrogen molecules

Fig. 6. The changes in the capacitance of the electrical double layer of anode during operation of the cell. The changes were determined for different carbon monoxide hydrogen stream concentration (post 30 mins): 125, 250, and 325 ppb.

and adsorption of hydrogen atoms on to platinum (Tafel reaction):

$$H_2 + Pt = 2(H)_{AD} Pt \tag{4}$$

Hydrogen dissociation on platinum may also be electrochemical (Heyrovsky reaction):

$$H_2 + Pt = (H)_{AD} Pt + H^+ + e^- \tag{5}$$

The adsorbed hydrogen is oxidized to release a hydrogen cation and an electron (Volmer reaction):

$$(H)_{AD} Pt = H^+ + e^- \tag{6}$$

The oxidation of hydrogen depends on the formation of an adsorbed atom, which has a key role in the reaction. The process occurs in a finite number of active sites on a platinum electrode.

In the presence of carbon monoxide near the electrode, regardless of whether the first step is the chemical dissociation (4) or electrochemical dissociation (5), on the active centres of the platinum electrode, there occurs a competitive process with CO adsorption:

$$CO + Pt = (CO)_{Ad} Pt \tag{7}$$

The adsorption of carbon monoxide is manifested by a reduction in the capacitance of the double electrical layer on the electrode surface. Fig. 6 shows the changes in the capacitance of the double electrical layer caused by the influence of carbon monoxide on the anode. For times close to the limit of zero, the capacity of the double layer reaches a limit value corresponding to the situation when there is no carbon monoxide in the system:

$$\lim_{t \to 0} C_{DL}^A(t) = C_{DL}^A(\theta = 0) = 3.03F \tag{8}$$

where: $C_{DL}^A(\theta = 0)$ – capacitance of electrical double layer of anode corresponding to the surface coverage $\theta = 0$.

For the highest concentrations of carbon monoxide, with varying exposure times, a new steady (stationary) state is reached. In this state, the limit of the capacitance of the anodic double layer is given as:

$$\lim_{t \to \infty} C_A(t) = C_{DL}^A(\theta = 1) = 0.22F \tag{9}$$

where: $C_{DL}^A(\theta = 1)$ – of electrical double layer of anode corresponding to the surface coverage $\theta = 1$.

This value of capacitance corresponds to a situation where all the active centres of the platinum catalyst are coated with adsorbed carbon monoxide molecules. Therefore, the rate of carbon monoxide adsorption drops to zero. According to the Frumkin formula, the surface coverage can be determined from measurements of double electrical layer. The surface coverage is given by the formula:

$$C_{DL}^A(\theta, t) = (1 - \theta) C_{DL}^A(\theta = 0) + \theta C_{DL}^A(\theta = 1) \tag{10}$$

$$\theta(t) = \frac{C_{DL}^A(\theta = 0) - C_{DL}^A(\theta, t)}{C_{DL}^A(\theta = 0) - C_{DL}^A(\theta = 1)} \tag{11}$$

where: $\theta(t)$ – surface coverage changing over time, $C_{DL}^A(\theta, t)$ - the double electrical layer capacitance corresponding to the surface coverage $\theta(t)$.

Associated issues with formula (10) may be caused by the hydrogen oxidation reaction taking place on the electrode. The course of reaction is related to the formation of the adsorbed intermediate products, thus, co-adsorption of $(H)_{AD}$ and $(CO)_{AD}$ occurs. However, &alert_message_var;CHECK CHARACTER NOT SUPPORTEDthe situation simplifies greatly when one realizes that the process runs with a direct current. The rate of hydrogen oxidation is constant and the value of surface coverage θ is also constant.&alert_message_var;CHECK CHARACTER NOT SUPPORTED &alert_message_var;CHECK CHARACTER NOT SUPPORTED&alert_message_var;CHECK CHARACTER NOT SUPPORTED

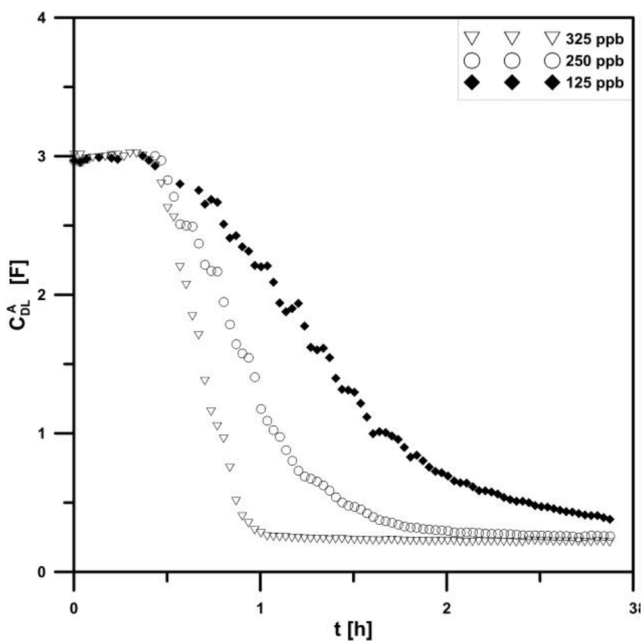The change in the surface coverage of CO over time is given as de-

rivative:

$$\frac{d\theta}{dt} = -\frac{1}{C_{DL}^A(\theta=0) - C_{DL}^A(\theta=1)} \frac{dC(\theta)}{dt} \quad (12)$$

The change in the surface coverage over time is related to the rate of carbon monoxide adsorption on the anode for given cell operating conditions. This is true for a specified current load and a specified content of CO in H$_2$ and constant experimental conditions. As it has been shown in Fig. 6, the curves for the varying capacitance of electrical double layer of anode may be directly linked with the changes in the surface coverage for CO adsorption over time (11). Fig. 7 shows the changes in surface coverage over time, determined for the specific content of CO in the hydrogen stream. By differentiating the surface coverage with respect to time, we derive the rate of adsorption. The values of $\frac{d\theta}{dt}$ for concentrations of 125, 250, and 325 ppb are $4.81\cdot10^{-08}$, $8.43\cdot10^{-08}$, and $1.58\cdot10^{-07}$ s^{-1}, respectively.

The adsorption of carbon monoxide should significantly increase the charge transfer resistance of the hydrogen oxidation. For different contents of carbon monoxide, the identified changes in charge transfer resistance for hydrogen oxidation is given in Fig. 8

An increase of carbon monoxide content in hydrogen increases the charge transfer resistance. For the maximum surface coverage, the charge transfer resistance can be extrapolated:

$$\lim_{t\to\infty} R_{CT}^A(t) = R_{CT}^A(\theta=1) \cong 4.5m\Omega \quad (13)$$

where: $R_{CT}^A(\theta=1) - $ the resistance of hydrogen oxidation corresponding to the anode being fully covered by adsorbed CO.

The extrapolated charge transfer resistance of hydrogen oxidation in the absence of carbon monoxide is given as:

$$\lim_{t\to0} R_{CT}^A(t) = R_{CT}^A(\theta=0) \cong 0.1m\Omega \quad (14)$$

where: $R_{CT}^A(\theta=0) - $ the resistance of the hydrogen oxidation in the absence of CO.

Both the double-layer capacitance and the charge transfer resistance of the hydrogen oxidation on platinum depend strongly on the surface coverage. It is worth noting that the changes in the surface coverage over

Fig. 8. The changes in the anodic charge transfer resistance during operation of the cell. The changes were determined for different carbon monoxide hydrogen stream concentrations (post 30 mins): 125, 250, and 325 ppb.

Fig. 9. The changes in the anodic charge transfer resistance as a function of the surface coverage. The changes were determined for different carbon monoxide content (post 30 mins) in the hydrogen stream: 125, 250, and 325 ppb.

time have been determined previously (Fig. 7). Based on this one can determine the relationship between the charge transfer resistance $R_{CT}^A(t)$ and the surface coverage for the concentrations of carbon monoxide. The relationship between the charge transfer resistance of the hydrogen oxidation for different concentrations of CO in the fuel stream and the degree of coverage is shown in Fig. 9.

With a low content, 125 and 250 ppb, of carbon monoxide in the hydrogen, no significant effect of the charge transfer resistance for hydrogen oxidation is observed. The inhibitory effect is negligible with surface coverage ranging from $0 < \theta < 0.80$. For surface coverage values greater than $\theta = 0.80$, the inhibitory effect manifests itself very clearly.
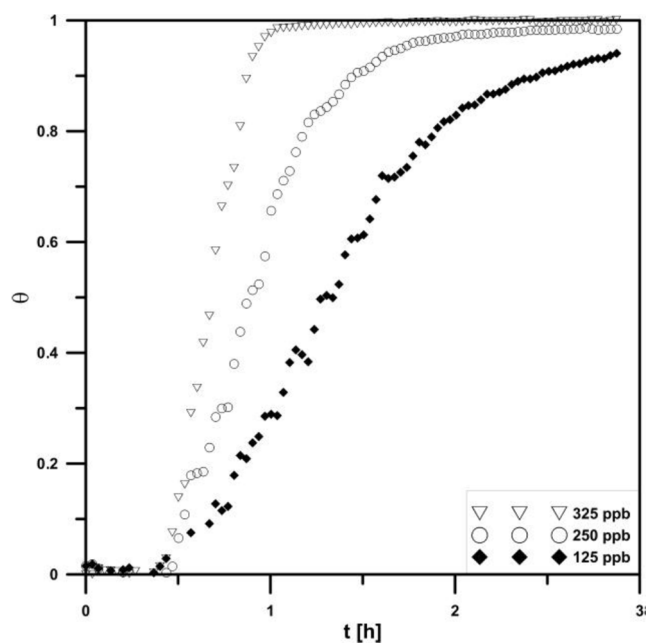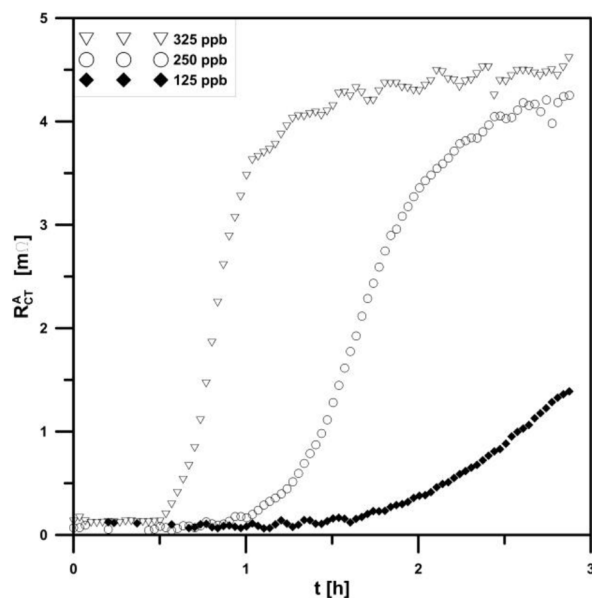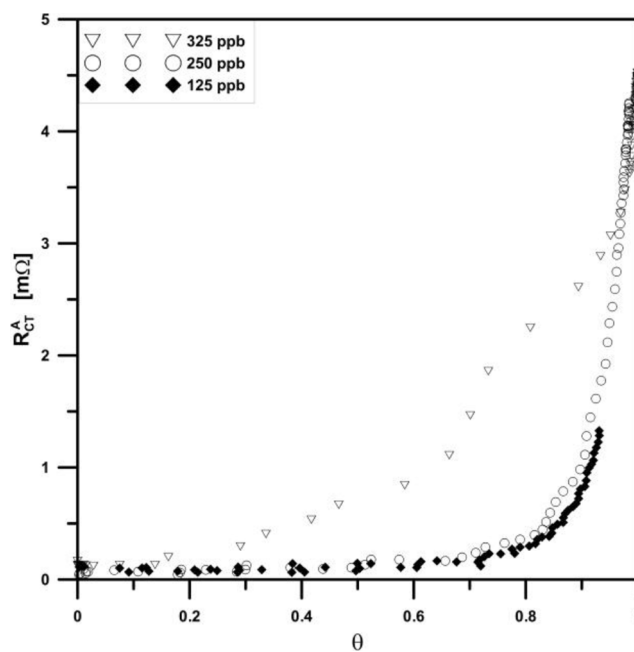

Fig. 7. The changes in the anodic surface coverage factor of the catalyst during operation of the cell. The changes were determined for different carbon monoxide hydrogen stream concentrations (post 30 mins) of: 125, 250, and 325 ppb.

6

The inhibitory effect occurs over the entire range of surface coverage values for the relatively high CO contamination, 325 ppb. In this case, the resistance of the hydrogen oxidation is subject to changes over the entire range of surface coverage variation.

Complete surface coverage by adsorbed carbon monoxide does not limit the course of hydrogen oxidation, meaning the reaction continues. But the resistance of the reaction increases by approximately forty times. Thus, inhibition of hydrogen oxidation by the adsorbed CO, among other things, limits the number of active centres available on platinum. The process is more complex and is associated with an increase in the free enthalpy of activation of the hydrogen oxidation, which is a function of the surface coverage.

3.4. Self-verification of the implemented procedure

The DEIS methodology allows one to measure impedance in galvanostatic conditions and simultaneously measure the constant voltage at the cell terminals, as expressed by:

$$U(t) = \Delta E_{rev} - i(R_\infty + R_M) - iR_{CT}^A(t) - iR_{CT}^C(t) - \eta_{gas}^{dry} - \eta_{gas}^{wet} \tag{15}$$

$$U(t) = E_C - E_A(t) \tag{16}$$

where E_{rev} is the difference of reversible thermodynamic potential depending on temperature and gas partial pressure, η_{gas}^{dry} is the gas diffusion overpotential controlled by the diffusion of oxygen and voltage losses from hydrogen diffusion are essentially negligible, and η_{gas}^{wet} are additional gas diffusion overpotential losses caused by the presence of liquid water in diffusion media.

Considering the constant stream of protons passing through the membrane from the anode to cathode and the constant stream of oxygen supplied to the cathode, the changes in voltage at the terminal of the cell are linked to changes in the hydrogen oxidation resistance. By differentiating equations (15 and 16), we obtain the following relationship:

$$\frac{dE_A(t)}{dt} = i\frac{dR_{CT}^A(t)}{dt} \tag{17}$$

This criterion being fulfilled is a clear confirmation that the analysis is valid.

Fig. 10 shows the changes in voltage between the cell terminals during the experiment for different concentrations of CO in the hydrogen stream. The increase in carbon monoxide content causes increasingly deep changes in voltage at the cell terminals, reaching up to 200 mV. This voltage drop in not acceptable for operating conditions. This causes a significant loss of power. However, the main reason for determining these characteristics is the self-verification of the measurements and analyses performed. Therefore, Fig. 11 was prepared to compare the rates of voltage changes and the rates of anodic overpotential changes.

The lines correspond to the rate of change in the anodic overpotential $i\frac{dR_{CT}^A(t)}{dt}$, whereas the points indicate the rate of change in the voltage $\frac{dE_A(t)}{dt}$, and the relationships coincide. This proves the validity of the proposed procedure used to determine the anode impedance. Direct-current measurements are directly correlated with the results for the alternating-current measurements. This is not possible for conventional impedance measurements, in which you can only determine the individual spectra using frequency-by-frequency methods.

4. Summary and conclusions

The achieved results show the significant influence of carbon monoxide, in the stream of hydrogen, on the anode impedance during the cell operation. Carbon monoxide at a concentration of 125 ppb marginally affects the performance of the anode. Contamination of the hydrogen feed with carbon monoxide at a concentration of 250 ppb or greater has a significant influence on anode impedance and decrease of the voltage at the cell's terminals. The impedance changes of the whole cell are directly caused by changes occurring at the cell's anode during the supply of fuel with different carbon monoxide concentrations. This level of testing has never been previously performed in a dynamic manner. Consequently, the testing with the use of Electrochemical Impedance Spectroscopy did not allow for clear identification of anode's impedance, or making credible the conclusions about the obtained trend of changes in the anodic parameters of the equivalent circuit during the exposure to carbon monoxide and determining the rates of changes over time was not possible. Therefore, the Dynamic Electrochemical Impedance Spectroscopy technique is an ideal tool for diagnosing and
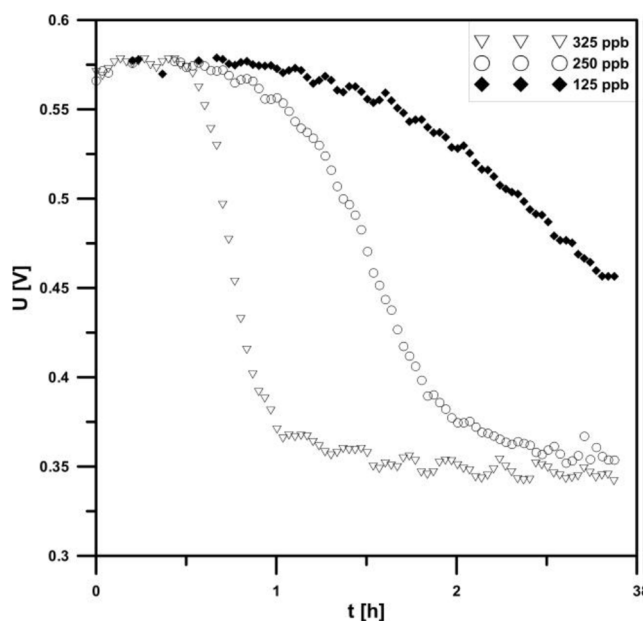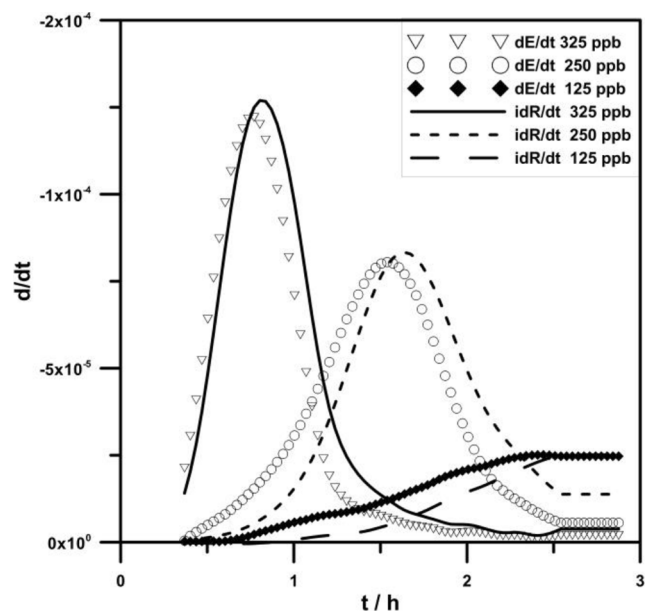

Fig. 10. The changes in the voltage during operation of the cell. The changes were determined for different carbon monoxide hydrogen stream concentrations (post 30 mins): 125, 250, and 325 ppb.

Fig. 11. The rate of change in cell voltage during operation compared to changes in the anodic overpotential, determined for different concentrations of carbon monoxide (post 30 mins) in the hydrogen stream with concentrations of 125, 250, and 325 ppb.

monitoring the condition of fuel cells under real, dynamic operating conditions, even when the level of hydrogen contamination by carbon monoxide is extremely low. The chrono-impedance plots do visibly evolve, reflecting changes in the anode during the exposure to carbon monoxide. The proposed procedure of limiting the number of independent variables in the correlation analysis led to the removal of the anode impedance. This allowed for monitoring of the anode condition over time. As expected, the higher the concentration of carbon monoxide in the fuel, the more dynamic the changes of the anode impedance. The rate of these changes can be expressed as function of $\frac{d\theta}{dt}$ and for concentrations of 125, 250, and 325 ppb are $4.81 \cdot 10^{-08}$, $8.43 \cdot 10^{-08}$, and $1.58 \cdot 10^{-07}$ s^{-1}, respectively. As the measurements show, the mechanism for inhibition of hydrogen oxidation is complex and is not limited by the reducing number of platinum active centres, on which hydrogen can be oxidised.

Typically, the results of the conventional impedance measurements are related to the analysis of the individual frequency spectra. Therefore, the analysis is based on various premises and is not always reliable. In contrast to this, a self-verification procedure has been proposed. The obtained consistency of DC and AC measurements prove the accuracy of the impedance analysis.

The conducted tests show that the developed procedures can be applied to evaluate the quality of the catalyst used and its sensitivity to poisoning even for low carbon oxide concentrations. Dynamic electrochemical impedance spectroscopy provided an excellent and unique representation of the dynamics of changes in the processes taking place on the anode. This, indeed, shows that Dynamic Electrochemical Impedance Spectroscopy has a high potential for application in online monitoring of fuel cells.

CRediT authorship contribution statement

K. Darowicki: Conceptualization, Methodology, Project administration, Funding acquisition. **L. Gawel:** Supervision, Conceptualization, Software, Validation, Formal analysis, Writing - original draft, Writing - review & editing, Visualization. **M. Mielniczek:** Investigation, Writing - review & editing. **A. Zielinski:** Software, Validation, Visualization. **E. Janicka:** Writing - original draft, Writing - original draft. **J. Hunger:** Resources, Writing - review & editing. **L. Jorissen:** Resources, Funding acquisition.

Declaration of Competing Interest

The authors declare that they have no known competing financial interests or personal relationships that could have appeared to influence the work reported in this paper.

Acknowledgements

References

[1] Wang Y, Chen KS, Mishler J, Cho SC, Adroher XC. A review of polymer electrolyte membrane fuel cells: Technology, applications, and needs on fundamental research. Appl Energy 2011;88:981–1007. https://doi.org/10.1016/j.apenergy.2010.09.030.

[2] Tang Y, Yuan W, Pan M, Li Z, Chen G, Li Y. Experimental investigation of dynamic performance and transient responses of a kW-class PEM fuel cell stack under various load changes. Appl Energy 2010;87:1410–7. https://doi.org/10.1016/j.apenergy.2009.08.047.

[3] Tang Y, Yuan W, Pan M, Wan Z. Experimental investigation on the dynamic performance of a hybrid PEM fuel cell/battery system for lightweight electric vehicle application. Appl Energy 2011;88:68–76. https://doi.org/10.1016/j.apenergy.2010.07.033.

[4] Robledo CB, Oldenbroek V, Abbruzzese F, van Wijk AJM. Integrating a hydrogen fuel cell electric vehicle with vehicle-to-grid technology, photovoltaic power and a residential building. Appl Energy 2018;215:615–29. https://doi.org/10.1016/j.apenergy.2018.02.038.

[5] Alavi F, Park Lee E, van de Wouw N, De Schutter B, Lukszo Z. Fuel cell cars in a microgrid for synergies between hydrogen and electricity networks. Appl Energy 2017;192:296–304. https://doi.org/10.1016/j.apenergy.2016.10.084.

[6] Guida D, Minutillo M. Design methodology for a PEM fuel cell power system in a more electrical aircraft. Appl Energy 2017;192:446–56. https://doi.org/10.1016/j.apenergy.2016.10.090.

[7] Belmonte N, Staulo S, Fiorot S, Luetto C, Rizzi P, Baricco M. Fuel cell powered octocopter for inspection of mobile cranes: Design, cost analysis and environmental impacts. Appl Energy 2018;215:556–65. https://doi.org/10.1016/j.apenergy.2018.02.072.

[8] Wagner N. Electrochemical Impedance Spectroscopy. In: Li H, editor. PEM Fuel Cell Diagnostic Tools, CRC Press; 2011, p. 37–70. 10.1201/b11100-5.

[9] Balasubramanian S, Weidner JW. Analysis of an Electrochemical Filter for Removing Carbon Monoxide from Reformate Hydrogen. J Electrochem Soc 2015; 162:E231–6. https://doi.org/10.1149/2.2081511jes.

[10] Springer TE, Rockward T, Zawodzinski TA, Gottesfeld S. Model for Polymer Electrolyte Fuel Cell Operation on Reformate Feed: Effects of CO, H₂ Dilution, and High Fuel Utilization. J Electrochem Soc 2001;148:A11. https://doi.org/10.1149/1.1344516.

[11] Wagner N, Schulze M. Change of electrochemical impedance spectra during CO poisoning of the Pt and Pt–Ru anodes in a membrane fuel cell (PEFC). Electrochim Acta 2003;48:3899–907. https://doi.org/10.1016/S0013-4686(03)00528-0.

[12] Postole G, Auroux A. The poisoning level of Pt/C catalysts used in PEM fuel cells by the hydrogen feed gas impurities: The bonding strength. Int J Hydrogen Energy 2011;36:6817–25. https://doi.org/10.1016/j.ijhydene.2011.03.018.

[13] Meland A-K, Kjelstrup S. Three steps in the anode reaction of the polymer electrolyte membrane fuel cell. Effect of CO. J Electroanal Chem 2007;610:171–8. https://doi.org/10.1016/j.jelechem.2007.07.008.

[14] Igarashi H, Fujino T, Watanabe M. Hydrogen electro-oxidation on platinum catalysts in the presence of trace carbon monoxide. J Electroanal Chem 1995;391: 119–23. https://doi.org/10.1016/0022-0728(95)03914-3.

[15] Watanabe M, Motoo S. Chemisorbed CO on a polycrystalline platinum electrode The effect of conditioning of the surface and of partial pressure of CO. J Electroanal Chem Interfacial Electrochem 1986;206:197–208. https://doi.org/10.1016/0022-0728(86)90268-8.

[16] Fasmin F, Ramanathan S. Effect of CO Poisoning of PEM Fuel Cell Anode on Impedance Spectra-Simulations. ECS Trans 2015;66:1–14. https://doi.org/10.1149/06627.0001ecst.

[17] Neugebohren J, Borodin D, Hahn HW, Altschäffel J, Kandratsenka A, Auerbach DJ, et al. Velocity-resolved kinetics of site-specific carbon monoxide oxidation on platinum surfaces. Nature 2018;558:280–3. https://doi.org/10.1038/s41586-018-0188-x.

[18] Zhang J, editor. PEM fuel cell electrocatalysts and catalyst layers: fundamentals and applications. London: Springer; 2008.

[19] Wang JX, Springer TE, Adzic RR. Dual-Pathway Kinetic Equation for the Hydrogen Oxidation Reaction on Pt Electrodes. J Electrochem Soc 2006;153:A1732. https://doi.org/10.1149/1.2218756.

[20] Kabbabi A, Faure R, Durand R, Beden B, Hahn F, Leger J-M, et al. In situ FTIRS study of the electrocatalytic oxidation of carbon monoxide and methanol at platinum–ruthenium bulk alloy electrodes. J Electroanal Chem 1998;444:41–53. https://doi.org/10.1016/S0022-0728(97)00558-5.

[21] Yamanaka T, Takeguchi T, Wang G, Muhamad EN, Ueda W. Particle size dependence of CO tolerance of anode PtRu catalysts for polymer electrolyte fuel cells. J Power Sour. 2010;195:6398–404. https://doi.org/10.1016/j.jpowsour.2010.04.007.

[22] Kadirgan F, Kannan AM, Atilan T, Beyhan S, Ozenler SS, Suzer S, et al. Carbon supported nano-sized Pt–Pd and Pt–Co electrocatalysts for proton exchange membrane fuel cells. Int J Hydrogen Energy 2009;34:9450–60. https://doi.org/10.1016/j.ijhydene.2009.09.028.

[23] Wendt H, Spinacé EV, Oliveira Neto A, Linardi M. Electrocatalysis and electrocatalysts for low temperature fuel cells: fundamentals, state of the art, research and development. Quím Nova 2005;28:1066–75. https://doi.org/10.1590/S0100-40422005000600023.

[24] Wee J-H, Lee K-Y. Overview of the development of CO-tolerant anode electrocatalysts for proton-exchange membrane fuel cells. J Power Sour. 2006;157: 128–35. https://doi.org/10.1016/j.jpowsour.2005.08.010.

[25] Gasteiger HA, Markovic NM, Ross PN. H2 and CO Electrooxidation on Well-Characterized Pt, Ru, and Pt-Ru. 1. Rotating Disk Electrode Studies of the Pure Gases Including Temperature Effects. J Phys Chem 1995;99:8290–301. https://doi.org/10.1021/j100020a063.

[26] Wang Z-B, Yin G-P, Shao Y-Y, Yang B-Q, Shi P-F, Feng P-X. Electrochemical impedance studies on carbon supported PtRuNi and PtRu anode catalysts in acid medium for direct methanol fuel cell. J Power Sour 2007;165:9–15. https://doi.org/10.1016/j.jpowsour.2006.12.027.

[27] Taniguchi A, Akita T, Yasuda K, Miyazaki Y. Analysis of electrocatalyst degradation in PEMFC caused by cell reversal during fuel starvation. J Power Sour 2004;130: 42–9. https://doi.org/10.1016/j.jpowsour.2003.12.035.

[28] Sheng W, Gasteiger HA, Shao-Horn Y. Hydrogen Oxidation and Evolution Reaction Kinetics on Platinum: Acid vs Alkaline Electrolytes. J Electrochem Soc 2010;157: B1529. https://doi.org/10.1149/1.3483106.

[29] Wang JX, Zhang Y, Capuano CB, Ayers KE. Ultralow charge-transfer resistance with ultralow Pt loading for hydrogen evolution and oxidation using Ru@Pt core-shell nanocatalysts. Sci Rep 2015;5:12220. https://doi.org/10.1038/srep12220.

[30] Nakajima H, Konomi T, Kitahara T, Tachibana H. Electrochemical Impedance Parameters for the Diagnosis of a Polymer Electrolyte Fuel Cell Poisoned by Carbon Monoxide in Reformed Hydrogen Fuel. J Fuel Cell Sci Technol 2008;5:041013. https://doi.org/10.1115/1.2931462.

[31] Tang Y, Zhang H, Zhong H, Xu Z. In-situ investigation on the CO tolerance of carbon supported Pd–Pt electrocatalysts with low Pt content by electrochemical impedance spectroscopy. Int J Hydrogen Energy 2012;37:2129–36. https://doi.org/10.1016/j.ijhydene.2011.10.104.

[32] Ciureanu M. Electrochemical Impedance Study of Electrode-Membrane Assemblies in PEM Fuel Cells: I. Electro-oxidation of H_2 and H_2/CO Mixtures on Pt-Based Gas-Diffusion Electrodes. J Electrochem Soc 1999;146:4031. https://doi.org/10.1149/1.1392588.

[33] Chandesris M, Guetaz L, Schott P, Scohy M, Escribano S. Investigation of Degradation Heterogeneities in PEMFC Stack Aged under Reformate Coupling In Situ Diagnosis, Post-Mortem Ex Situ Analyses and Multi-Physic Simulations. J Electrochem Soc 2018;165:F3290–306. https://doi.org/10.1149/2.0321806jes.

[34] Yuan X, Wang H, Colinsun J, Zhang J. AC impedance technique in PEM fuel cell diagnosis—A review. Int J Hydrogen Energy 2007;32:4365–80. https://doi.org/10.1016/j.ijhydene.2007.05.036.

[35] Pivac I, Barbir F. Inductive phenomena at low frequencies in impedance spectra of proton exchange membrane fuel cells – A review. J Power Sour 2016;326:112–9. https://doi.org/10.1016/j.jpowsour.2016.06.119.

[36] Wu J, Yuan X, Wang H, Blanco M, Martin J, Zhang J. Diagnostic tools in PEM fuel cell research: Part I Electrochemical techniques. Int J Hydrogen Energy 2008;33: 1735–46. https://doi.org/10.1016/j.ijhydene.2008.01.013.

[37] Giner-Sanz JJ, Ortega EM, Pérez-Herranz V. Mechanistic equivalent circuit modelling of a commercial polymer electrolyte membrane fuel cell. J Power Sources 2018;379:328–37. https://doi.org/10.1016/j.jpowsour.2018.01.066.

[38] Darowicki K, Orlikowski J, Lentka G. Instantaneous impedance spectra of a non-stationary model electrical system. J Electroanal Chem 2000;486:106–10. https://doi.org/10.1016/S0022-0728(00)00111-X.

[39] Darowicki K, Ślepski P. Dynamic electrochemical impedance spectroscopy of the first order electrode reaction. J Electroanal Chem 2003;547:1–8. https://doi.org/10.1016/S0022-0728(03)00154-2.

[40] Darowicki K, Ślepski P. Influence of the analyzing window on electrode impedance measurement by the continuous frequency scanning method. J Electroanal Chem 2002;533:25–31. https://doi.org/10.1016/S0022-0728(02)01085-9.

[41] Darowicki K, Janicka E, Mielniczek M, Zielinski A, Gawel L, Mitzel J, et al. The influence of dynamic load changes on temporary impedance in hydrogen fuel cells, selection and validation of the electrical equivalent circuit. Appl Energy 2019;251: 113396. https://doi.org/10.1016/j.apenergy.2019.113396.

[42] Janicka E, Mielniczek M, Gawel L, Darowicki K, Landowska P. The impact of air humidity on the operation of proton exchange membrane fuel cells determined using dynamic electrochemical impedance spectroscopy. Electrochim Acta 2020; 341:136036. https://doi.org/10.1016/j.electacta.2020.136036.

[43] Darowicki K, Janicka E, Mielniczek M, Zielinski A, Gawel L, Mitzel J, et al. Implementation of DEIS for reliable fault monitoring and detection in PEMFC single cells and stacks. Electrochim Acta 2018. https://doi.org/10.1016/j.electacta.2018.09.105.

[44] Slepski P, Darowicki K, Janicka E, Lentka G. A complete impedance analysis of electrochemical cells used as energy sources. J Solid State Electrochem 2012;16: 3539–49. https://doi.org/10.1007/s10008-012-1825-1.

[45] Slepski P, Janicka E, Darowicki K, Pierozynski B. Impedance monitoring of fuel cell stacks. J Solid State Electrochem 2015;19:929–33. https://doi.org/10.1007/s10008-014-2676-8.

[46] Darowicki K, Gawel L. Impedance Measurement and Selection of Electrochemical Equivalent Circuit of a Working PEM Fuel Cell Cathode. Electrocatalysis 2017;8: 235–44. https://doi.org/10.1007/s12678-017-0363-0.

[47] Slepski P, Darowicki K, Janicka E, Sierczynska A. Application of electrochemical impedance spectroscopy to monitoring discharging process of nickel/metal hydride battery. J Power Sour 2013;241:121–6. https://doi.org/10.1016/j.jpowsour.2013.04.039.

[48] Slepski P, Janicka E. A comprehensive analysis of impedance of the electrochemical cell. Russ J Electrochem 2014;50:379–84. https://doi.org/10.1134/S1023193513090103.

[49] Singh RK, Devivaraprasad R, Kar T, Chakraborty A, Neergat M. Electrochemical Impedance Spectroscopy of Oxygen Reduction Reaction (ORR) in a Rotating Disk Electrode Configuration: Effect of Ionomer Content and Carbon-Support. J Electrochem Soc 2015;162:F489–98. https://doi.org/10.1149/2.0141506jes.

[50] Paulus UA, Schmidt TJ, Gasteiger HA, Behm RJ. Oxygen reduction on a high-surface area Pt/Vulcan carbon catalyst: a thin-film rotating ring-disk electrode study. J Electroanal Chem 2001;495:134–45. https://doi.org/10.1016/S0022-0728(00)00407-1.

[51] Song C, Tang Y, Zhang JL, Zhang J, Wang H, Shen J, et al. PEM fuel cell reaction kinetics in the temperature range of 23–120°C. Electrochim Acta 2007;52: 2552–61. https://doi.org/10.1016/j.electacta.2006.09.008.

[52] Wagner N, Friedrich KA. FUEL CELLS – PROTON-EXCHANGE MEMBRANE FUEL CELLS | Dynamic Operational Conditions. Encyclopedia Electrochem Power Sour Elsevier 2009:912–30. https://doi.org/10.1016/B978-044452745-5.00239-2.